ABSTRACT

JEONG, CHANG WOO. Interfacial Phenomena on Polymeric Thin Films. (Under the direction of Dr. Orlando J. Rojas).

Model thin films relevant to various biomaterials applications were used to investigate the interfacial phenomena that occur on polymeric surfaces. Quartz Crystal Microbalance with Dissipation (QCM-D) was used to investigate conformational change of soft materials, adsorption and desorption kinetics of macromolecules and interaction between absorbates and model surfaces. Specifically, this thesis deals with enzymatic activity on thin films of cellulose of lignin, and salt- induced changes for surface-grafted neutral thermoresponsive polymers.

It was possible to study *in situ* and in real time the dynamics of enzymatic activity with the QCM-D. After an initial phase, which was controlled by enzyme binding on the substrate, an increase in the resonant frequency of the sensor was apparent. This increase of frequency was explained by the reduction in effective mass due to enzymatic degradation. The rate at which this degradation occurs was found to depend strongly on the enzyme concentration, temperature and the pH of the solution as well as the mixing conditions within the reaction cell.

QCM-D was also employed to estimate the effect of salt on the volume phase transition of thermoresponsive polymer brushes. Changes in mass and viscoelasticity of grafted poly (N-isopropyl acrylamide) (PNIPAM) layers grafted from QCM-D sensors were measured as a function of temperature, upon contact with aqueous solutions of variable salt concentration. The phase transition temperature of PNIPAM brushes, $T_{C,graft}$, quantified by using the QCM-

D was reduced with increases in the concentration of salt. This phenomenon is explained by the tendency of salt ions to affect structure of water molecules (Hofmeister effect).

The investigation on changes in the hydrophlicity of milled wood lignin films were studied by QCM-D and static contact angle mesurements. After laccase incubation, significant decrease in resonant frequency and increase in energy dissipation was observed. It was demonstrated that the film became less hydrophobic due to the oxidation by laccase. Overall, this thesis demonstrates the potential of QCM-D to characterize the detailed kinetics of enzyme activity and to monitor the conformational changes of polymer brushes grafted on the surface of QCM resonator.

INTERFACIAL PHENOMENA ON POLYMERIC THIN FILMS

by
CHANG WOO JEONG

A thesis submitted to the Graduate Faculty of
North Carolina State University
In partial fulfillment of the
Requirement for the Degree of
Master of Science

WOOD AND PAPER SCIENCE

Raleigh

2006

APPROVED BY:

_____ _____

_____
Chair of Advisory Committee

BIOGRAPHY

Chang Woo Jeong was born on December 1, 1975 in Busan, Korea. In February of 2002, he obtained a Bachelor of Science degree in Forest Resources and Environmental Science at Korea University, Seoul, Korea. In August of 2003, he started his Master of Science in Wood and Paper Science, North Carolina State University, College of Natural Resources. His interest involves colloid and surface chemistry and dynamics of enzyme activity.

ACKNOWLEDGEMENTS

The author would like to express his best gratitude to his advisor, Dr. Orlando J. Rojas for not only advising him on the technical matters with regard to his research but also supporting his new life here in the U.S. He also would like to express his appreciation to his committee members, Dr. Dimitris S. Argyropoulos and Dr. Martin A. Hubbe for supporting the research project by giving valuable advice and scientific ideas. In particular, the author appreciates all the advices and discussion that Dr. Ana M. Maciel offered during AFM training and technical support. He is very grateful to his friends in the Department of Wood and Paper Science, especially Junlong Song, Denny Hu, Sayong Lee, Sunkyu Park, Jungmyung Lee, and Dr. Jooyoun Kim. Their assistance encouraged and inspired him to continue improving himself and spend a fulfilling time at NC State University. Also, he wishes to thank all the faculty, instructors, and staff who shared precious experiences with him while at NC State University.

Finally, he wishes to thank his wife and family for their continuing support and encouragement throughout his life.

TABLE OF CONTENTS

LIST OF TABLES

LIST OF FIGURES

Chapter. 2 Following cellulase activity by the Quartz Crystal Microbalance technique.

Chapter 1. INTRODUCTION

QCM-D is a state-of-the-art instrument which takes advantage of the piezoelectric phenomenon of quartz crystals. Quartz resonators have been used to elucidate the swelling behavior of cellulose in solution with different salt concentrations [1], conformational changes of polymer or polyelectrolytes [2-4], the adsorption kinetics of polymers [5], polyelectrolytes [6-8] and surfactants [9-11] under different conditions. Also, viscoelastic properties on multilyer films [12], the kinetics of polymer brush growth [13], and the efficiency of enzyme immobilization have been studied by using this technique[14]. QCM-D also has been utilized in biotechnology and medical applications such as immunoassay using antigen and antibody [15-17]; hemocompatibility of biomaterials [18, 19]; DNA assembly and hybridization reaction [20], and lipid bilayers as model cell membrane [21-26]. Energy dissipation is a unique surface property that has added new dimensions to our knowledge in soft matter behavior such as interactions between aqueous solution [27, 28], proteins [29], polymers [30] and hydrogels and adsorption of proteins on synthetic polymers [31-33], modified surfaces [34-36] and interaction between proteins [37].

A stable model surface with a defined chemistry, topography and swelling degree is necessary to obtain deeper understanding on the chemical nature of cellulose and lignin. During the last decade, several attempts have been made to prepare model surfaces from cellulose [38-42].

While the only milled wood lignin film was reported by Tammelin *et al* [43].

In the case of thermosensitive polymer brush, the active side of the cuartz crystal was coated with a thin layer (≈50 nm) of silicon oxide. PNIPAM chains were grafted from this layer of

silicon oxide using atom transfer radical polymerization (ATRP). Thickness of PNIPAM on QCM crystal was estimated by growing PNIPAM brushes simultaneously on a reference silicon wafer and measuring the dry thickness of the polymer layer (≈15nm) by ellipsometry. Of all, in this research, enzyme dynamics on thin films of lignin and cellulose and, the phase transition behavior of thermoresponsive polymer brushes (PNIPAM) were monitored with piezoelectric sensors via QCM-D.

References

[1] S. Falt, L. Wagberg, and E. L. Vesterlind, "Swelling of model films of cellulose having different charge densities and comparison to the swelling behavior of corresponding fibers," *Langmuir*, vol. 19, pp. 7895-7903, 2003.

[2] S. M. Notley, S. Biggs, V. S. J. Craig, and L. Wagberg, "Adsorbed layer structure of a weak polyelectrolyte studied by colloidal probe microscopy and QCM-D as a function of pH and ionic strength," *Physical Chemistry Chemical Physics*, vol. 6, pp. 2379-2386, 2004.

[3] G. M. Liu and G. Z. Zhang, "Reentrant behavior of poly(N-isopropylacrylamide) brushes in water-methanol mixtures investigated with a quartz crystal microbalance," *Langmuir*, vol. 21, pp. 2086-2090, 2005.

[4] M. T. Muller, X. P. Yan, S. W. Lee, S. S. Perry, and N. D. Spencer, "Lubrication properties of a brushlike copolymer as a function of the amount of solvent absorbed within the brush," *Macromolecules*, vol. 38, pp. 5706-5713, 2005.

[5] T. Kallio, J. Kekkonen, and P. Stenius, "The formation of deposits on polymer surfaces in paper machine wet end," *Journal of Adhesion*, vol. 80, pp. 933-969, 2004.

[6] M. A. Plunkett, P. M. Claesson, M. Ernstsson, and M. W. Rutland, "Comparison of the adsorption of different charge density polyelectrolytes: A quartz crystal microbalance and X-ray photoelectron spectroscopy study," *Langmuir*, vol. 19, pp. 4673-4681, 2003.

[7] M. A. Plunkett, P. M. Claesson, and M. W. Rutland, "Adsorption of a cationic polyelectrolyte followed by surfactant-induced swelling, studied with a quartz crystal microbalance," *Langmuir*, vol. 18, pp. 1274-1280, 2002.

[8] J. Iruthayaraj, E. Poptoshev, A. V. Vareikis, R. Makuska, A. van der Wal, and P. M. Claesson, "Adsorption of low charge density polyelectrolyte containing poly(ethylene oxide) side chains on silica: Effects of ionic strength and pH," *Macromolecules*, vol. 38, pp. 6152-6160, 2005.

[9] J. Merta, T. Tammelin, and P. Stenius, "Adsorption of complexes formed by cationic starch and anionic surfactants on quartz studied by QCM-D," *Colloids and Surfaces a-Physicochemical and Engineering Aspects*, vol. 250, pp. 103-114, 2004.

[10] K. Boschkova, A. Feiler, B. Kronberg, and J. J. R. Stalgren, "Adsorption and frictional properties of gemini surfactants at solid surfaces," *Langmuir*, vol. 18, pp. 7930-7935, 2002.

[11] M. Knag, T. Tammelin, K. Bilkova, L. S. Johansson, E. Gulbrandsen, and J. Sjoblom, "Adsorption of polycation and anionic surfactant onto iron surfaces and the inhibition of carbon dioxide corrosion," *Journal of Dispersion Science and Technology*, vol. 27, pp. 277-292, 2006.

[12] S. M. Notley, M. Eriksson, and L. Wagberg, "Visco-elastic and adhesive properties of adsorbed polyelectrolyte multilayers determined in situ with QCM-D and AFM measurements," *Journal of Colloid and Interface Science*, vol. 292, pp. 29-37, 2005.

[13] S. E. Moya, A. A. Brown, O. Azzaroni, and W. T. S. Huck, "Following polymer brush growth using the quartz crystal microbalance technique," *Macromolecular Rapid Communications*, vol. 26, pp. 1117-1121, 2005.

[14] X. D. Su, Y. Zong, R. Richter, and W. Knoll, "Enzyme immobilization on poly (ethylene-co-acrylic acid) films studied by quartz crystal microbalance with dissipation monitoring," *Journal of Colloid and Interface Science*, vol. 287, pp. 35-42, 2005.

[15] A. Sellborn, M. Andersson, J. Hedlund, J. Andersson, M. Berglin, and H. Elwing, "Immune complement activation on polystyrene and silicon dioxide surfaces Impact of reversible IgG adsorption," *Molecular Immunology*, vol. 42, pp. 569-574, 2005.

[16] S. D. Carrigan, G. Scott, and M. Tabrizian, "Real-time QCM-D immunoassay through oriented antibody immobilization using cross-linked hydrogel biointerfaces," *Langmuir*, vol. 21, pp. 5966-5973, 2005.

[17] S. D. Carrigan, G. Scott, and M. Tabrizian, "Rapid three-dimensional biointerfaces for real-time immunoassay using hIL-18BPa as a model antigen," *Biomaterials*, vol. 26, pp. 7514-7523, 2005.

[18] T. P. Vikinge, K. M. Hansson, P. Sandstrom, B. Liedberg, T. L. Lindahl, I. Lundstrom, P. Tengvall, and F. Hook, "Comparison of surface plasmon resonance and quartz crystal microbalance in the study of whole blood and plasma coagulation," *Biosensors & Bioelectronics*, vol. 15, pp. 605-613, 2000.

[19] M. Andersson, J. Andersson, A. Sellborn, M. Berglin, B. Nilsson, and H. Elwing, "Quartz crystal microbalance-with dissipation monitoring (QCM-D) for real time measurements of blood coagulation density and immune complement activation on artificial surfaces," *Biosensors & Bioelectronics*, vol. 21, pp. 79-86, 2005.

[20] X. D. Su, Y. J. Wu, and W. Knoll, "Comparison of surface plasmon resonance spectroscopy and quartz crystal microbalance techniques for studying DNA assembly and hybridization," *Biosensors & Bioelectronics*, vol. 21, pp. 719-726, 2005.

[21] S. Svedhem, D. Dahlborg, J. Ekeroth, J. Kelly, F. Hook, and J. Gold, "In situ peptide-modified supported lipid bilayers for controlled cell attachment," *Langmuir*, vol. 19, pp. 6730-6736, 2003.

[22] B. Seantier, C. Breffa, O. Felix, and G. Decher, "In situ investigations of the formation of mixed supported lipid bilayers close to the phase transition temperature," *Nano Letters*, vol. 4, pp. 5-10, 2004.

[23] I. Reviakine, F. F. Rossetti, A. N. Morozov, and M. Textor, "Investigating the properties of supported vesicular layers on titanium dioxide by quartz crystal microbalance with dissipation measurements," *Journal of Chemical Physics*, vol. 122, 2005.

[24] B. Seantier, C. Breffa, O. Felix, and G. Decher, "Dissipation-enhanced quartz crystal microbalance studies on the experimental parameters controlling the formation of supported lipid bilayers," *Journal of Physical Chemistry B*, vol. 109, pp. 21755-21765, 2005.

[25] S. Boudard, B. Seantier, C. Breffa, G. Decher, and O. Felix, "Controlling the pathway of formation of supported lipid bilayers of DMPC by varying the sodium chloride concentration," *Thin Solid Films*, vol. 495, pp. 246-251, 2006.

[26] R. P. Richter, J. L. K. Him, B. Tessier, C. Tessier, and A. R. Brisson, "On the kinetics of adsorption and two-dimensional self-assembly of annexin A5 on supported lipid bilayers," *Biophysical Journal*, vol. 89, pp. 3372-3385, 2005.

[27] M. S. Lord, M. H. Stenzel, A. Simmons, and B. K. Milthorpe, "Lysozyme interaction with poly(HEMA)-based hydrogel," *Biomaterials*, vol. 27, pp. 1341-1345, 2006.

[28] P. Asberg, P. Bjork, F. Hook, and O. Inganas, "Hydrogels from a water-soluble zwitterionic polythiophene: Dynamics under pH change and biomolecular interactions observed using quartz crystal microbalance with dissipation monitoring," *Langmuir*, vol. 21, pp. 7292-7298, 2005.

[29] M. S. Lord, M. H. Stenzel, A. Simmons, and B. K. Milthorpe, "The effect of charged groups on protein interactions with poly(HEMA) hydrogels," *Biomaterials*, vol. 27, pp. 567-575, 2006.

[30] S. D. Carrigan and M. Tabrizian, "Reducing nonspecific adhesion on cross-linked hydrogel platforms for real-time immunoassay in serum," *Langmuir*, vol. 21, pp. 12320-12326, 2005.

[31] S. Thorslund, J. Sanchez, R. Larsson, F. Nikolajeff, and J. Bergquist, "Bioactive heparin immobilized onto microfluidic channels in poly(dimethylsiloxane) results in hydrophilic surface properties," *Colloids and Surfaces B-Biointerfaces*, vol. 46, pp. 240-247, 2005.

[32] E. Gurdak, C. C. Dupont-Gillain, J. Booth, C. J. Roberts, and P. G. Rouxhet, "Resolution of the vertical and horizontal heterogeneity of adsorbed collagen layers by combination of QCM-D and AFM," *Langmuir*, vol. 21, pp. 10684-10692, 2005.

[33] E. F. Irwin, J. E. Ho, S. R. Kane, and K. E. Healy, "Analysis of interpenetrating polymer networks via quartz crystal microbalance with dissipation monitoring," *Langmuir*, vol. 21, pp. 5529-5536, 2005.

[34] A. Welle, "Competitive plasma protein adsorption on modified polymer surfaces monitored by quartz crystal microbalance technique," *Journal of Biomaterials Science-Polymer Edition*, vol. 15, pp. 357-370, 2004.

[35] D. E. Otzen, M. Oliveberg, and F. Hook, "Adsorption of a small protein to a methyl-terminated hydrophobic surfaces: effect of protein-folding thermodynamics and kinetics," *Colloids and Surfaces B-Biointerfaces*, vol. 29, pp. 67-73, 2003.

[36] A. G. Hemmersam, M. Foss, J. Chevallier, and F. Besenbacher, "Adsorption of fibrinogen on tantalum oxide, titanium oxide and gold studied by the QCM-D technique," *Colloids and Surfaces B-Biointerfaces*, vol. 43, pp. 208-215, 2005.

[37] J. Limson, O. O. Odunuga, H. Green, F. Hook, and G. L. Blatch, "The use of a quartz crystal microbalance with dissipation for the measurement of protein-protein interactions: a qualitative and quantitative analysis of the interactions between molecular chaperones," *South African Journal of Science*, vol. 100, pp. 678-682, 2004.

[38] R. D. Neuman, B. J.M., and C. P.M., "Direct measurement of surface forces in papermaking and paper coating systems," *Nordic Pulp and Paper Research Journal*, vol. 8, pp. 96-104, 1993.

[39] M. Holmberg, R. Wigren, R. Erlandsson, and P. M. Claesson, "Interactions between cellulose and colloidal silica in the presence of polyelectrolytes," *Colloids and Surfaces a-Physicochemical and Engineering Aspects*, vol. 130, pp. 175-183, 1997.

[40] J. F. Revol, L. Godbout, and D. G. Gray, "Solid self-assembled films of cellulose with chiral nematic order and optically variable properties," *Journal of Pulp and Paper Science*, vol. 24, pp. 146-149, 1998.

[41] L. H. Torn, "Polymers and surfactants in solution and at interfaces," Wageningen University, 2000.

[42] S. Gunnars, L. Wagberg, and M. A. C. Stuart, "Model films of cellulose: I. Method development and initial results," *Cellulose*, vol. 9, pp. 239-249, 2002.

[43] T. Tammelin, M. Osterberg, S. T., L. S. Johansson, and J. Laine, "Development of model surfaces for different pulp fibre components," presented at 13th ISWFPC, Auckland, 2005.

Chapter 2.

Following Cellulase Activity by the Quartz Crystal Microbalance Technique

ABSTRACT

In this investigation we examined the interfacial behavior of cellulase active enzymes on model cellulose substrates. By using the Quartz Crystal Microbalance with Dissipation monitoring (QCM-D) it was possible to study in situ and in real time the dynamics of enzymatic activity. After an initial phase, which is controlled by the adsorption of the enzyme on the surface, an increase in the resonant frequency of the crystal was apparent. This increase of frequency indicates the degradation of the film due to the enzymatic activity. Our work has demonstrated that the rate at which this degradation occurs depends on the enzyme concentration, temperature and the pH of the solution as well as the mixing conditions within the reaction cell.

Overall, this paper demonstrates for the first time the potential of QCM-D to characterize and monitor the detailed kinetics of enzyme activity on cellulosic substrates, adding another dimension to our knowledge and to the methods available for such enquiries.

INTRODUCTION

Cellulose and hemicellulose can be converted to soluble sugars by enzyme hydrolysis. The main enzymes, cellulase and hemicellulase are primarily derived from microbial origins. Cellulases hydrolyze the β-1-4 linkages between glucose moieties found in cellulose to produce lower molecular weight polysaccharides and eventually glucose. These enzymes are

of current commercial significance in detergent formulations to remove cellulosic stains [1] and in processing textiles to create specialty fabrics such as stone washed jeans [2]. In recent years they have been used as a pulp pretreatment to reduce the amount of chemical required to bleach pulps for white papers [3]. Potential uses of cellulases in the pulp and paper industry include the improvement of drainage, the reduction of pitch problems, de-inking, and reduction of power consumption in refining operations [3-5].

Cellulases

Microorganisms including fungi (e.g., brown or white rot fungi) and bacteria produce various types of cellulase components. In some cases, genetic material is transferred to a host organism for commercial production. Because the original organism evolved to metabolize a mixed substrate containing cellulose, hemicelluloses, lignin, and extractives the lower cost commercial enzymes are often a mixture of different specific isozymes.

Commercial cellulase mixes usually contain one or more exoglucanases such as cellobiohydrolase (CBH), which will proceed from either the reducing end or non reducing end of the cellulose chain and produce a shortened chain and cellobiose. The cellulase mixture may also contain several endoglucanases (EGI, EGII, etc), which cleave randomly the internal β-1,4-glycosidic bonds of the cellulose chain along its length to produce free chain ends that will be acted upon by exoglucanases. Most cellulases also contain both β-glucosidase, which hydrolyzes cellobiose units to glucose monomers, and various hemicellulases, which may have side chain cleaving capabilities. For complete hydrolysis of

cellulosic material the synergistic combination of endoglucanase, exoglucanase, and β-glucosidase is required [6].

Cellulosic Substrates

Interactions of cellulases with cellulose play an important role in determining the efficiency of the enzymatic hydrolysis [7,8]. Therefore, an understanding of enzyme interactions with substrates is of great importance in processing wood and cellulosic fibers.

The rate of enzymatic hydrolysis and its yield are dependent on the adsorption of enzyme onto the substrate surface. The accessibility of cellulose to the cellulase seems to be controlled by the physicochemical properties of the substrate [9,10], the multiplicity of the cellulase complex [11], and reaction parameters such mass transfer [12] and temperature [10]. Various kinetic models have been developed to describe the hydrolysis rate of cellulase. The models are based on parameters such as the amount of adsorbed enzyme on the cellulose surface [13], the structural characteristics of the substrate including pore size distribution, crystallinity index, and specific surface [14,15], and cellulase-cellulose adsorption rate [16-18].

The mechanism of adsorption of most cellulase components onto cellulose is still unknown as well as the role of the different structural domains in cellulase action and their effects on substrates. Furthermore, with complex mixtures it can be difficult to understand how to dose enzymes to provide the correct level of activity. Often dosage rates are arrived at empirically based on a supposedly constant activity. Most current activity assay methods use a particular

substrate such as filter paper or carboxymethylcellulose. In this investigation, the use of a piezoelectric sensor, the Quartz Crystal Microbalance (QCM), is proposed to monitor, in situ and in real time, the catalytic activity of cellulases on model substrates.

EXPERIMENTAL

Materials and Methods

The enzyme used in this work was a commercially-available multi-component cellulase (Rocksoft^{TM} ACE P150, Dyadic Int., FL). Sodium bicarbonate, sodium hydroxide, hydrochloric acid and acetic acid (all from Fisher Scientific), sodium acetate trihydrate (Fluka) and tris (hydroxymethyl) aminomethane (Acros) were used in the preparation of the buffer solutions of pH 4.5, 7 and 10. Water was obtained from a Milli-Q® Gradient system (resistivity >18MΩ).

Cellulose Thin Films and Related Methods

Cellulose thin films were used as models for cellulose. The process for preparing these surfaces [19] starts with either silicon wafers or QCM-D electrodes which are cleaned by standard chemical treatment and UV-ozone plasma. The QCM-D electrodes consisted of quartz crystals (Q-sense) coated with a conductive gold layer and a top 50-nm silica layer.

Cellulose solution was prepared by dissolving micro-crystalline cellulose (MCC) in 50 %wt water/N-Methylmorpholine-N-oxide (NMMO) at 115 ^{o}C. DMSO was added to adjust the concentration of cellulose (0.05%) in the mixture. The cellulose solution was then spin coated (Laurell Technologies model WS-400A-6NPP) on the substrates (silica wafer or

QCM electrodes) at 5000 rpm for 40 seconds. The substrate was removed from the spin coater and placed in a milli-Q water bath to precipitate the cellulose. The cellulose-coated substrate was then washed thoroughly with milli-Q water, dried in a vacuum oven at 40 ºC and stored at room temperature in a clean chamber for further use.

Cellulose Characterization

Ellipsometry, X-ray Photoelectron Spectroscopy (XPS), and Atomic Force Microscopy (AFM) were used to characterize the cellulose films. XPS was performed on bare silicon, PVAm, and cellulose-coated wafers to quantify the respective chemical composition. This was accomplished by using a RIBER LAS-3000 XPS system with Mg Kα (1253.6 eV) as X-ray source. The thin cellulose films were characterized in terms of material distribution, surface roughness and topography using a Q-Scope 250 AFM (Quesant Inst. Corp.), before or prior to enzyme treatment. The scans were performed in dried conditions using NSC16 standard wavemode Si_3N_4 tips with a force
constant of 40 N/m (according to the manufacturer) and a typical resonant frequency of 170±20kHz. Finally, a Rudolph single-wavelength ellipsometer was used to determine the thickness of cellulose films on the surface of the silicon wafers (a refractive index of cellulose film was taken as 1.56).

Enzyme/Cellulose Surface Interactions

Quartz Crystal Microbalance

A Quartz Crystal Microbalance with Dissipation monitoring, QCM-D (Q-sense D-300, Sweden) was used to study enzyme binding and activity on cellulose thin films deposited on quartz/gold electrodes which are coated with a 50 nm SiO_2 layer.

QCM-D consists of a thin plate of a piezoelectric quartz crystal, sandwiched between a pair of electrodes. It measures simultaneously changes in resonance frequency, *f*, and dissipation, *D* (the frictional and viscoelastic energy losses in the system), due to adsorption on a crystal surface. *f* is measured before disconnecting the driving oscillator, and *D* is obtained by suddenly disconnecting the driving field and recording the damped oscillating signal as its vibration amplitude decays exponentially. Mechanical stress causes electric polarization in a piezoelectric material. The converse effect refers to the deformation of the same material by applying an electric field. Therefore, when an AC voltage is applied over the electrodes the crystal can be made to oscillate. Resonance is obtained when the thickness of the plate is an odd integer, *n*, of half wavelengths of the induced wave, *n* being an integer since the applied potential over the electrodes is always in anti-phase. If something is adsorbed onto the crystal, it can be treated as an equivalent mass change of the crystal itself. The increase in mass,*m*, induces a proportional shift in frequency, *f*. This linear relationship between *m* and *f* was for the first time demonstrated by Sauerbrey [20]

$$\Delta m = \frac{-\rho_q t_q \Delta f}{f_0 n} = \frac{-\rho_q v_q \Delta f}{2 f_0^2 n} = -\frac{C \Delta f}{n} \qquad (1)$$

where ρ_q and v_q are the specific density and the shear wave velocity in quartz respectively; t_q is the thickness of the quartz crystal, and f_0 the fundamental resonance frequency (when n =1). For the crystal used in these measurements the constant C has a value of 17.8 ng cm^{-2} Hz^{-1}. The relation is valid when the following conditions are fulfilled: (i) the adsorbed mass is distributed evenly over the crystal. (ii) Δm is much smaller than the mass of the crystal itself (<1%), and (iii) the adsorbed mass is rigidly attached, with no slip or inelastic deformation in the added mass due to the oscillatory motion. The last condition is valid when the frequency decreases in proportion to the true mass of the adsorbate with no change in energy dissipation. Variations in the energy dissipation upon adsorption thus reflect the energy dissipation in the adlayer or at its interface. We note that the mass detected with the QCM-D device includes any change in the amount of solvent that oscillates with the surface. This quantity may be significant for extended layers and thus one expects to obtain a higher value for the adsorbed amount from QCM-D studies than from, e.g., ellipsometry.

The Dissipation (D) Factor

A film that is "soft" (viscoelastic) will not fully couple to the oscillation of the crystal. The dissipation factor is proportional to the power dissipation in the oscillatory system and can give valuable information about the rigidity of the film:

$$D = \frac{E_{dissipated}}{2\pi E_{stored}} \qquad (2)$$

Here $E_{\text{dissipated}}$ is the energy dissipated during one oscillation and E_{stored} is the energy stored in the oscillating system. Hence, the measured change in D is due to changes in contributions from, e.g., slip and viscous losses. For QCM measurements in liquids, the major contribution to D comes from frictional (viscous) losses within the liquid contacting the crystal. According to Stockbridge [21], the shift in dissipation factor in a liquid environment is:

$$\Delta D = \frac{1}{\rho_q t_q}\sqrt{\frac{\rho_l \eta_l}{2\pi f}} \qquad (3)$$

where η_l and ρ_l are the viscosity and density of the fluid, respectively, and t and ρ are the thickness and the density of the quartz plate. When the adsorbed film slips on the electrode, frictional energy is created that increases the dissipation. Furthermore, if the film is viscous, energy is also dissipated due to the oscillatory motion induced in the film (internal friction in the film). Hence, a rigid adsorbed layer gives no change in dissipation while a loose layer gives a dissipation increase.

Open and Close QCM Modes

Enzyme treatments were carried out using three different concentrations of the commercial enzyme in 50mM sodium acetate buffer (0.005, 0.00167 and 0.00056 solids %) in combination with different conditions of pH (4.5, 7 and 10) and temperature (28, 33 and 38 °C).

First, deaerated (vacuum pump) buffer solution (no enzyme present) was injected into the QCM cell in which a cellulose-covered QCM electrode was installed. At least 18 hours were allowed for the cellulose to fully swell in the respective buffer solution. After this stage, enzyme solution was continuously introduced into the QCM cell with a syringe pump (Cole-Parmer 74900 series) at a flow rate of 0.2 ml/min (*open mode*). Alternative experiments were performed in *batch* conditions. In the *batch mode* the enzyme solution was introduced in the cell making sure that the buffer solution that was initially present was fully displaced. No further (continuous) enzyme injection was allowed. In both the *open* and *close* modes, the enzyme solution was injected only after the drift of the third overtone frequency (f_3) was lower than 2 Hz/hr (for the buffer solution). After the respective enzyme treatment, the run was terminated when the change of frequency (f_3) was lower than 1Hz/5min.

RESULTS AND DISCUSSION

Substrate Characterization

Results from ellipsometry measurements on the PVAm/cellulose-coated substrates indicated a PVAm and cellulose layer thicknesses of ca. 1 and 12 nm, respectively. AFM height obtained after an incision on the cellulose thin film with a scalpel gave similar thickness value (10-16 nm). A typical AFM image for the cellulose thin film can be seen in *Fig. 1*. Line profiles showed a relatively uniform and homogeneous cellulose surface.

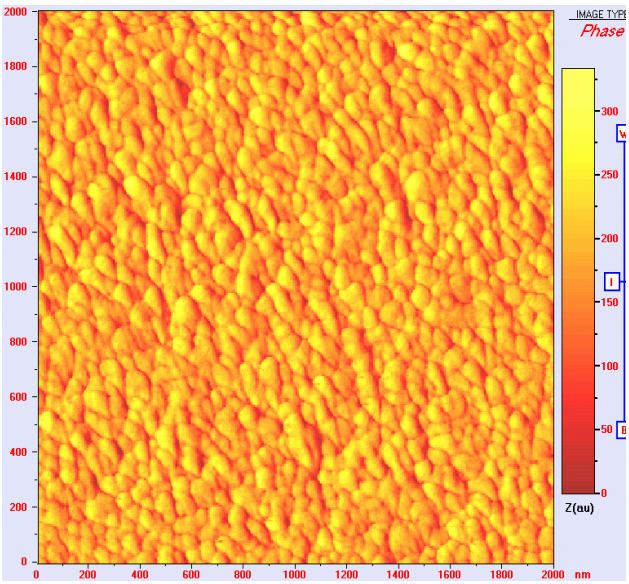

Figure 1. 2x2-µm AFM scan of cellulose thin film spin-coated on a silica wafer (wavemode image in dry conditions)

Chemical composition was confirmed by using XPS after curve fitting N and C peaks for the PVAm- and cellulose-coated silica surfaces. The ratio of O–C–O and C–O peaks was in agreement with the expected values obtained from the chemical composition of pure cellulose.

Enzymatic Degradation of Cellulose Films

Figure 2 shows a typical plot of QCM frequency and dissipation signal for a cellulose film subject to enzyme treatment. The adsorption of the enzyme onto the cellulose surface is clearly shown in the form of a (transient) reduction in the QCM-D frequency. Enzyme binding occurs rather fast (less than 5 min in most cases). After binding, a reduction in mass of material on the surface is observed as judged by the increase in oscillation frequency.

After some long time, the frequency signal reaches a plateau which indicates no further change in the mass of the film.

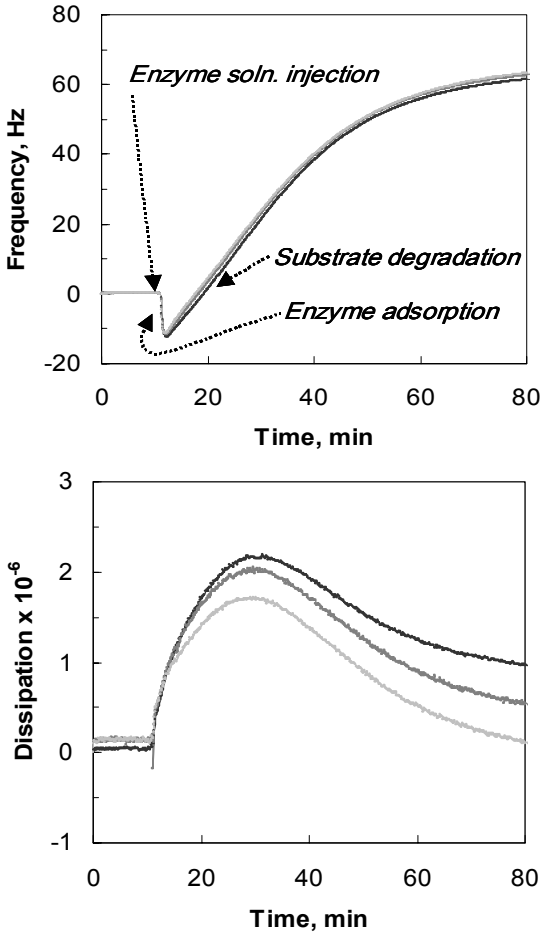

Figure 2. Change in frequency and dissipation by enzymatic degradation of cellulose thin films in cellulase solution (38 °C, 0.005% enzyme concentration and pH 4.5). The experiment was conducted in batch mode. The different lines represent the different overtones (harmonics): $f_3/3$ (black line), $f_5/5$ (medium gray) and $f_7/7$ (light grey). The driving frequencies correspond to 15, 25 and 35 MHz for f_3, f_5 and f_7, respectively.

Replacement of the enzyme solution by buffer solution (rinsing) did not produce any noticeable change in the frequency response (data not shown). This indicates that there is no further change in the adsorbed mass and also that the possible effect of variations in bulk density and viscosity is negligible.

The QCM dissipation seen in *Fig. 2* (bottom curves) mirror the behavior observed for the frequency, except for an initial dip after injecting enzyme solution (after 10 minutes operation) that we attribute to changes in temporal excess flow pressure on the crystal. Initially (< 10 min) the dissipation response for the buffer solution at the various overtones (D_3, D_5 and D_7) are very similar. This reveals the existence of an initial thin, relatively rigid, film of cellulose. After about 10 min of enzyme solution injection (at ca. 20 min run time), the energy dissipation starts to decrease and more distinctive differences for the different overtones are observed. This indicates structural changes in the cellulose film upon enzyme attack.

Confirmatory AFM imaging clearly indicates the effect of the enzyme treatment (see *Fig. 3*) as judged by the features observed before and after enzyme incubation. The characteristic "globular" features initially observed on the cellulose surface are largely reduced (or absent) after enzyme attack. The contrast between the AFM images of an area that was purposely scratched to expose the silica surface and the area covered by cellulose film serves as an "internal" verification of the topographical changes upon enzyme activity.

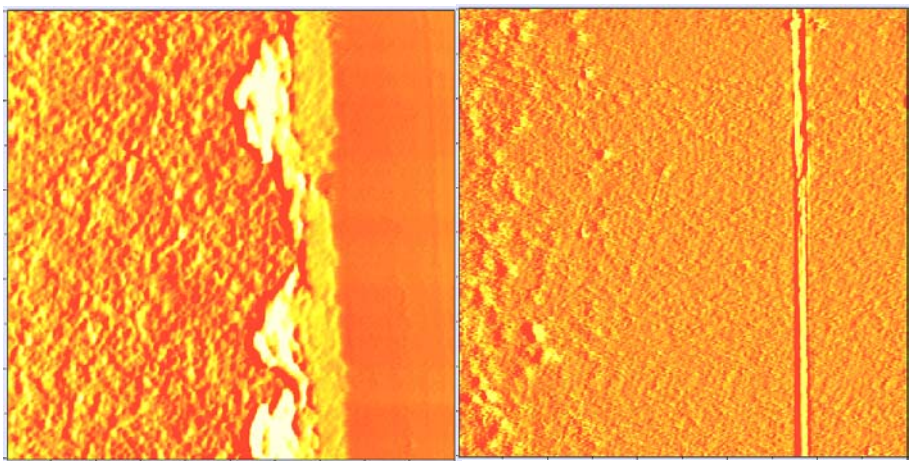

Figure 3. 5x5µm wavemode AFM image of a cellulose film before (left) and after (right) 2h incubation in commercial cellulase solution (38 °C, 0.005% enzyme concentration and pH 4.5). Note the enzyme treatment dissolved most of the features on the cellulose surface. A scratch on the surface was made to better distinguish structural changes in the film (see vertical feature on the right of each image).

Effect of Temperature

The frequency changes upon enzymatic degradation of cellulose films by cellulase under different temperature condition (38, 33 and 28 °C) and fixed concentration (0.005%) and pH (4.5) in both close and open modes are shown in *Fig 4*. Note that in the QCM instrument the temperature can be controlled within +/- 0.02 °C and the allowable range of operation ranges from 15 to 40 °C.

The catalytic activity of cellulase is taken as the initial slope of the curve after completion of enzyme binding. That is, the slope after the dip in the curve (before 20 min incubation time)

is directly related to the (initial) maximum rate of degradation. By comparing the different initial slopes at different temperatures, it can be concluded that in both, the close and open modes, the temperature plays a significant role in enzyme activity. It is clearly demonstrated that as the system is operated closer to the suggested optimal temperature (50 °C according to the manufacturer) there is an increase in the rate of enzymatic hydrolysis.

By comparing the two modes of operation, it is also possible to conclude that the mass exchange also plays an important role. This issue will be discussed in later sections. In AFM images (*Fig. 5*), most of the features on the cellulose film (selected for comparison purposes) were dissolved after the enzyme treatment. The RMS and average height values were also reduced considerably after the treatment.

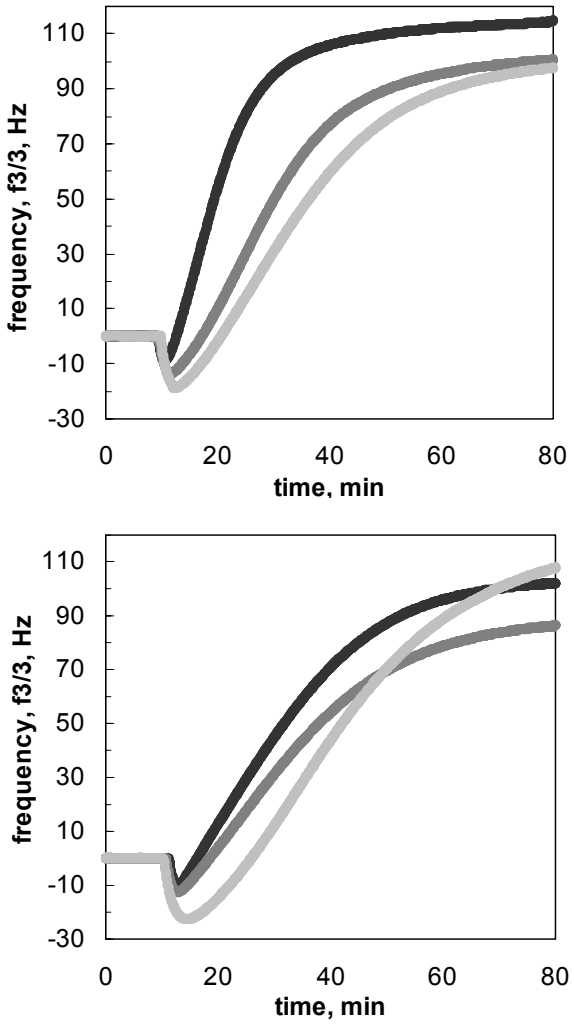

Figure 4. Change of crystal frequency (f3/3) after incubation of cellulose thin films in cellulase solutions (0.005%, pH 4.5) at three different temperatures: 38°C (black line), 33°C (medium grey) and 28°C (light gray). QCM driving frequency was 15 MHz and flow types were close (top) and open (bottom) modes.

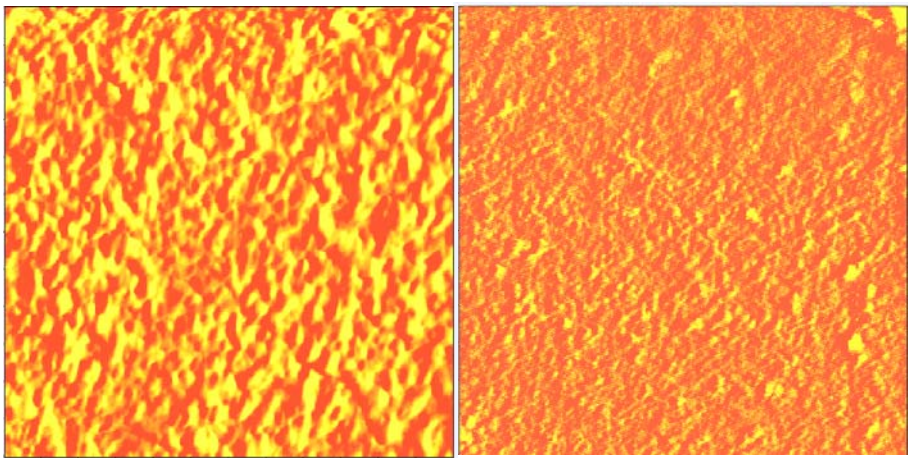

Figure 5. AFM image representing the same area of a cellulose thin film scanned to 3μm (X-Y) before and after 2h treatment at 38°C with cellulase solution at 0.005%. RMS and average height values reduced considerably after the enzyme treatment. Wavemode images were obtained in dried conditions using the Q-scope 250.

Effect of pH

The pH of the buffer solution affected significantly the initial rate of cellulose hydrolysis as can be observed in *Fig. 6* for frequency plots at three different pHs. Enzyme inactivation was observed at pH 10, as judged by the lack of change in frequency in this condition. More precisely, at pH 10 some minimal adsorption of the enzyme is observed on cellulose (frequency reduction), but no increase of frequency with time is observed. Unlike the case of pH 10, the use of cellulase at neutral and acidic pH shows (i) a distinctive adsorption (binding) step followed by (ii) cellulose degradation (increase in frequency).

The effect of pH on cellulose activity can be explained by the hydrogen ion concentration in the system. Interactions between the ionizable groups of both the substrate and the active site of the enzyme can induce the optimal condition for enzymatic degradation. The effect of the buffer solution pH is rather significant [22]. It is clearly observed that the initial rate of hydrolysis is distinctively larger for acidic conditions. This observation is well documented in the literature, where a low pH is recommended for higher hydrolysis rates [23].

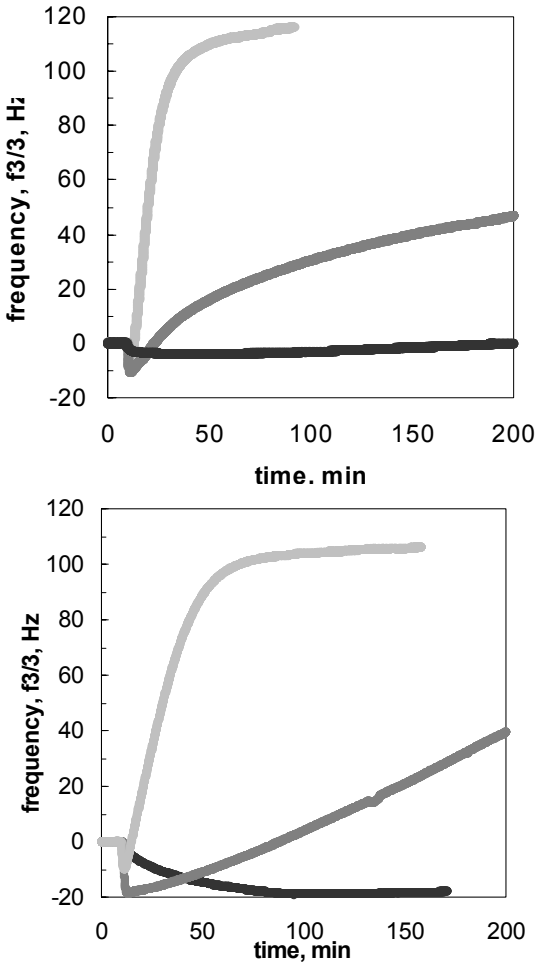

Figure 6. Change of QCM crystal frequency (f3/3) after incubation of cellulose thin films in cellulase solutions (0.005%, 38°C) at three different pHs: 10 (black line), 7 (medium grey) and 4.5 (light gray). QCM driving frequency was 15 MHz and flow types were close (top) and open (bottom) modes.

Effect of Cellulase Concentration

The enzymatic activity increased with the concentration of enzyme in buffer solution (see *Fig. 7*). At the lowest enzyme concentration studied (0.00056 %) both the binding and the rate of hydrolysis are very slow. This was confirmed by AFM imaging, where it is evident that the topography of the surface of the cellulose film remained somewhat similar after the enzyme treatment. The RMS and average height values were reduced slightly (see *Fig. 8*).

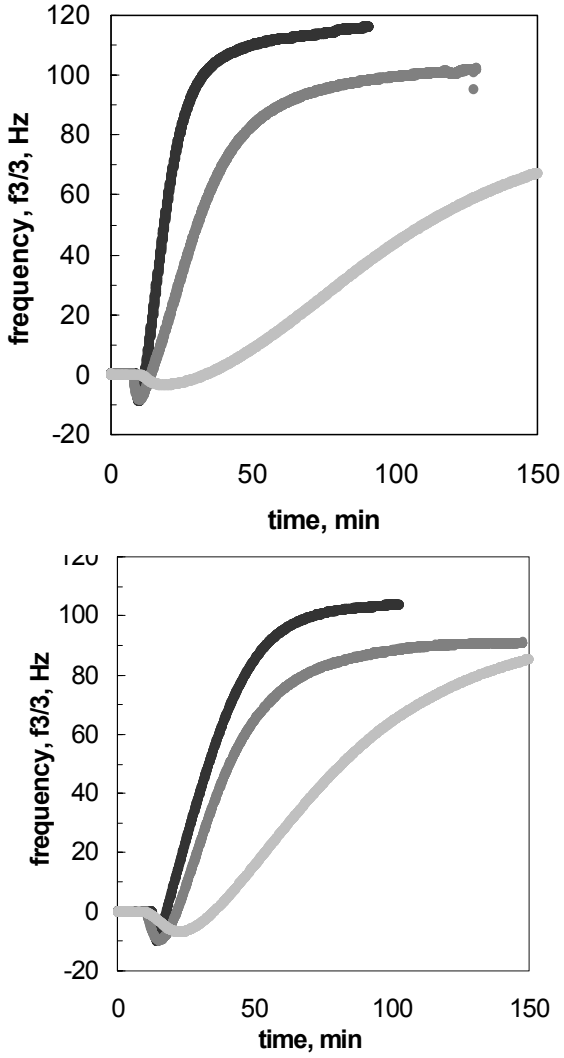

Figure 7. Change of QCM crystal frequency (f3/3) after incubation of cellulose thin films in cellulase solutions (pH 4.5, 38°C) at three different concentrations: 0.005 %, (black line), 0.00167 %(medium grey) and 0.00056 % (light gray). QCM driving frequency was 15 MHz and flow types were close (top) and open (bottom) modes.

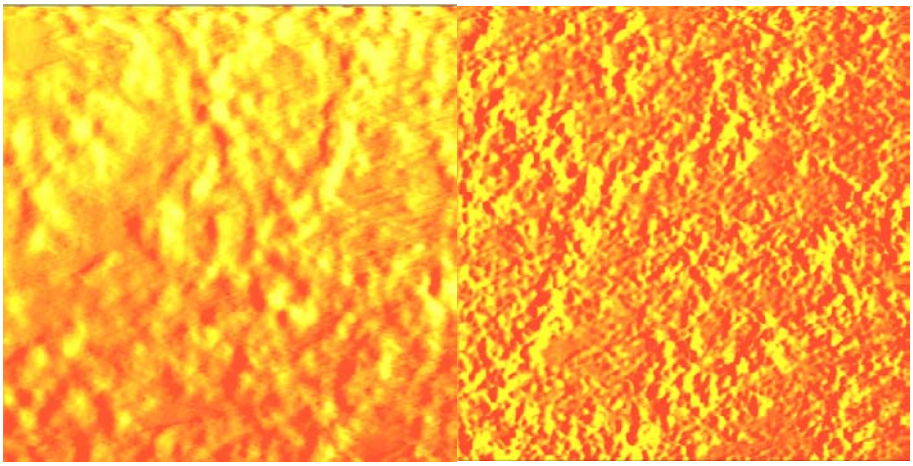

Figure 8. AFM image illustrating the same area of a cellulose film scanned to 3μm (X-Y) before and after the cellulase treatment to a minimum concentration of 0.0005 % and incubated at standard conditions. The RMS values were slightly reduced after the enzyme treatment.

Dynamics and Energetics of Enzyme Activity

Kinetic parameters of enzymatic degradation can be estimated by using QCM-D by comparing the initial slope of frequency vs. time curves. Table 1 shows the effect of the different conditions of temperature, pH and enzyme concentration on the initial reaction rates. These numbers summarize most of the data recorded in Figures 4, 6 and 7 and represent a simple way to estimate the activity of enzyme under different conditions of operation.

Table 1: Initial reaction rates from QCM slope in Close Mode (CM) and Open Mode (OM) enzyme injection.

Initial slope (Hz/min)			
		CM	OM
Temperature ^{o}C	28	3.29	2.74
	33	3.74	2.75
	38	7.38	3.40
pH	4.5	7.38	3.40
	7	0.94	0.27
	10	0.02	0.01
Concentration $x10^{3}$, %	5	7.38	3.40
	1.67	3.21	2.78
	0.56	0.25	0.89

All of the kinetic models developed so far assume that the initial rate of hydrolysis is proportional to the amount of enzyme-substrate complex formed by adsorption of cellulase. However, the proportional hydrolysis rate rapidly decreases with reaction time due to thermal instability of the cellulases [24]. It is also argued that the inactivation of the adsorbed cellulase is due to its diffusion into the cellulose fibrils [25]. However, in our experiments this effect can be ruled out, as the existence of fibrils is minimal. It is more likely that the inactivation of enzyme with time is related (at least in our case) with a strong inhibition by the by-products of hydrolysis, namely, cellobiose and glucose [26] and also by the transformation of the cellulose into less digestible forms [27]. In future work, QCM experiments will be conducted to test the effect of the crystallinity of the surface on enzyme activity, since it is anticipated that the cellulose micro-structure plays a significant role [28].

It is worth mentioning the differences in the initial rate of hydrolysis as obtained by the two operational modes, i.e., close and open modes. The reaction rate was consistently observed to

be higher for the close mode, which indicates that the controlling step in the dynamics of enzymatic reactions is not related to mass transport but rather to the cellulose-substrate binding. Furthermore, this observation was confirmed by operating at different flow rates (data not reported). Therefore, in the application of cellulase formulations, special attention needs to be paid to the presence of binding factors that facilitate adsorption and interaction with the cellulose surface. Cellulose-binding domains (CBD) improve the process for the reasons explained above.

The activation energy, E_a, of the enzymatic hydrolysis of cellulose can be estimated from the reaction constant (k) at different temperatures by using an Arrhenius expression. Even though no specific model was used to obtain the reaction constants, it can be argued that the initial rates of hydrolysis are directly related to the slopes of the QCM frequency vs. time curves. Any factor that is to be used to obtain the actual film mass is likely to be a linear function of frequency, as seen in the Sauerbrey Eq. (1). Furthermore, any contributing factor will cancel out if one takes the ratio of two QCM slopes at two different temperatures, and as a result it is possible to obtain E_a. Preliminary results by using this approach resulted in values of E_a in good agreement with data reported for cellulose/cellulase systems [29]. Therefore, not only our proposed QCM test is valuable to qualitatively describe the enzymatic degradation, but the results can be further expanded to obtain a quantitative assessment of cellulase activity. Work with a more extensive matrix of experimental conditions is underway to further explore issues related to kinetic models, rate constants and activation energies.

Overall, due to the complexity of the system, it is difficult to completely understand the enzymatic degradation of cellulose. The enzymatic activity in multi-component cellulases makes this even more difficult. The possibility of using in situ and real time detection with tools like the QCM justify more extensive efforts in this area.

CONCLUSIONS

A QCM technique to assay the activity of cellulase, based on the change in frequency during enzymatic degradation, was performed with cellulose thin films. The advantage of this technique is its simplicity and the ability to monitor enzyme activity in situ and real time. The initial slope in frequency-time curves is related to the initial reaction rates and is effective to estimate enzyme performance under different conditions of temperature, pH and concentration. It was demonstrated that the pH of the enzyme solution plays a key role for an optimum enzyme activity. Mass transport effects are also relevant and they can be easily judged by changing the flow rates in the QCM cell. AFM imaging was useful in comparing the changes produced in surface topography at different incubation conditions and allowed us to confirm our findings with the QCM.

REFERENCES

1. Ito, S. Alkaline cellulases from alkaliphilic Bacillus: Enzymatic properties, genetics, and application to detergents. *Extremophiles* **1**(2): 61-66 (1997).

2. Clarkson, K.A.;Swanson, B.Winetzky, D., USA Patent No. US Patent # 6,451,063 (September 17, 2002 2002).

3. Bajpai, A.;P.K., B.R., K. **Biotechnology for Environmental Protection in the Pulp and Paper Industry**: Springer, NY (1999).

4. Bajpai, P. **Enzymes in Pulp and Paper Processing**: Miller Freeman Inc., NY, 47-69. (1997).

5. Wong, K.K.Y.Mansfield, S.D. Enzymatic processing for pulp and paper manufacture - a review. *Appita Journal* **52**(6): 409-418 (1999).

6. Vinzant, T.B.;Adney, W.S.;Decker, S.R.;Baker, J.O.;Kinter, M.T.;Sherman, N.E.;Fox, J.W.Himmel, M.E. Fingerprinting Trichoderma reesei hydrolases in a commerical cellulase preparation. *Applied Biochemistry and Biotechnology* **91-3**: 99-107 (2001).

7. Tomme, P.;Vantilbeurgh, H.;Pettersson, G.;Vandamme, J.;Vandekerckhove, J.;Knowles, J.;Teeri, T.Claeyssens, M. Studies of the Cellulolytic System of Trichoderma-Reesei Qm-9414 - Analysis of Domain Function in 2 Cellobiohydrolases by Limited Proteolysis. *European Journal of Biochemistry* **170**(3): 575-581 (1988).

8. Gerber, P.J.;Joyce, T.W.;Heitmann, J.A.;Siika-Aho, M.Buchert, J. Adsorption of a Trichoderma reesei endoglucanase and cellobiohydrolase onto bleached Kraft fibres. *Cellulose* **4**(4): 255-268 (1997).

9. Lee, S.B.;Shin, H.S.;Ryu, D.D.Y.Mandels, M. Adsorption of Cellulase on Cellulose - Effect of Physicochemical Properties of Cellulose on Adsorption and Rate of Hydrolysis. *Biotechnology and Bioengineering* **24**(10): 2137-2153 (1982).

10. Ooshima, H.;Sakata, M.Harano, Y. Adsorption of Cellulase from Trichoderma-Viride on Cellulose. *Biotechnology and Bioengineering* **25**(12): 3103-3114 (1983).

11. Klyosov, A.A.;Mitkevich, O.V.Sinitsyn, A.P. Role of the Activity and Adsorption of Cellulases in the Efficiency of the Enzymatic-Hydrolysis of Amorphous and Crystalline Cellulose. *Biochemistry* **25**(3): 540-542 (1986).

12. Sakata, M.;Ooshima, H.Harano, Y. Effects of Agitation on Enzymatic Saccharification of Cellulose. *Biotechnology Letters* **7**(9): 689-694 (1985).

13. Ghose, T.K.Bisaria, V.S. Studies on the Mechanism of Enzymatic-Hydrolysis of Cellulosic Substances. *Biotechnology and Bioengineering* **21**(1): 131-146 (1979).

14. Grethlein, H.E. The Effect of Pore-Size Distribution on the Rate of Enzymatic-Hydrolysis of Cellulosic Substrates. *Bio-Technology* **3**(2): 155-160 (1985).

15. Fan, L.T.;Lee, Y.H.Beardmore, D.H. Mechanism of the Enzymatic-Hydrolysis of Cellulose - Effects of Major Structural Features of Cellulose on Enzymatic-Hydrolysis. *Biotechnology and Bioengineering* **22**(1): 177-199 (1980).

16. Stuart, J.Y.Ristroph, D.L. Analysis of Cellulose Cellulase Adsorption Data - a Fundamental Approach. *Biotechnology and Bioengineering* **27**(7): 1056-1059 (1985).

17. Lee, Y.H.Fan, L.T. Kinetic-Studies of Enzymatic-Hydrolysis of Insoluble Cellulose - Analysis of the Initial Rates. *Biotechnology and Bioengineering* **24**(11): 2383-2406 (1982).

18. Steiner, W.;Sattler, W.Esterbauer, H. Adsorption of Trichoderma-Reesei Cellulase on Cellulose - Experimental-Data and Their Analysis by Different Equations. *Biotechnology and Bioengineering* **32**(7): 853-865 (1988).

19. Gunnars, S.;Wagberg, L.Stuart, M.A.C. Model films of cellulose: I. Method development and initial results. *Cellulose Chemistry and Technology* **9**(3-4): 239 (2002).

20. Rodahl, M.;Hook, F.;Krozer, A.;Brzezinski, P.Kasemo, B. Quartz crystal microbalance setup for frequency and Q-factor measurements in gaseous and liquid environments. *Review of Scientific Instruments* **66**(7): 3924-3930 (1995).

21. Stockbridge, C.D. **Vacuum Microbalance Technique:** Plenum Press, New York (1966).

22. Deng, S.P.Tabatabai, M.A. Cellulose activity of soils. *Soli Biol. Biochem* **26**: 1347-1354 (1994).

23. Criquet, S. Measurement and characterization of cellulase activity in sclerophyllous forest litter. *Journal of Microbiological Methods* **50**(2): 165-173 (2002).

24. Caminal, G.;Lopezsantin, J.Sola, C. Kinetic Modeling of the Enzymatic-Hydrolysis of Pretreated Cellulose. *Biotechnology and Bioengineering* **27**(9): 1282-1290 (1985).

25. Tanaka, M.;Ikesaka, M.;Matsuno, R.Converse, A.O. Effect of Pore-Size in Substrate and Diffusion of Enzyme on Hydrolysis of Cellulosic Materials with Cellulases. *Biotechnology and Bioengineering* **32**(5): 698-706 (1988).

26. Holtzapple, M.T.;Caram, H.S.Humphrey, A.E. Determining the Inhibition Constants in the Hch-1 Model of Cellulose Hydrolysis. *Biotechnology and Bioengineering* **26**(7): 753-757 (1984).

27. Lee, Y.H.Fan, L.T. Kinetic-Studies of Enzymatic-Hydrolysis of Insoluble Cellulose .2. Analysis of Extended Hydrolysis Times. *Biotechnology and Bioengineering* **25**(4): 939-966 (1983).

28. Wald, S.;Wilke, C.R.Blanch, H.W. Kinetics of the Enzymatic-Hydrolysis of Cellulose. *Biotechnology and Bioengineering* **26**(3): 221-230 (1984).

29. He, D.;Bao, L.;Long, Y.;Wei, W.Yao, S. A new study of the enzymatic hydrolysis of carboxymethyl cellulose with a bulk acoustic wave sensor. *Talanta* **50**(6): 1267-1273 (2000).

Chapter 3.

Monitoring swelling effect of model lignin thin film by laccase incubation

Introduction

Lignins are composed of complex polymers containing aromatic groups. Lignin is considerably resistant to microbial degradation compared to cellulose and hemicellulose. Nevertheless, white-rot fungi such as *Trametes Versicolor, Phlebia Radiate, Marasmius quercophilus* etc. are known as microorganisms for degradation.

The applications of the laccases have been to increase the production of fuel ethanol from renewable raw materials [1], to remove the phenols from white grape [2,3] and to improve the efficiency of particular bioremediation processes [4,5]. One of the applications of the laccases has been used for the preparation of pulp. Degradation mechanisms of model lignin compounds such as a nonphenolic β-O-4 lignin dimer and biphenyl lignin by laccase from *Trametes Versicolor* were investigated [6-8]. However, the influence of laccase on a milled wood lignin (MWL) model surface has not been investigated. In this research, the use of Quartz Crystal Microbalance was proposed to monitor the lignin surface with laccase treatment.

Materials and Methods

Enzyme solution

The laccase used in this study was commercial laccase 20units/mg (Fluka) from Trametes Versicolor. Sodium acetate trihydrate (Fluka), sodium bicarbonate, sodium hydroxide and

acetic acid (all from Fisher Scientific) were used in the preparation of pH 4.5 and pH 10 buffer solutions. Water was obtained from a Milli-Q® Gradient system (resistivity >18MΩ). 1-Hydrobenzotriazole, HBT (Sigma-Aldrich) was used mediator diluted in pH 4.5 buffer (10mM). Enzyme solution consisted of 1mM HBT and 25ppm laccase in pH 4.5 buffer.

Atomic force microscopy (AFM)

The thin lignin films were characterized for surface roughness and topography by using a Q-Scope 250 AFM (Quesant Inst. Corp.). The scans were performed in dried conditions using NSC16 standard wavemode Si_3N_4 tips with a force constant of 40 N/m (according to the manufacturer) and a typical resonant frequency of 170±20kHz.

Preparation of polystyrene film

Polystyrene (PS) (Mw 230,000 g/mol, Mn 140,000 g/mol, Tg = 94℃; Sigma-Aldrich) was dissolved in toluene solution (99.5% ACS reagent, Sigma-Aldrich). A 0.5% PS solution was spreaded on QCM-D Au sensor (q-sense) and spinning conditions (Laurell Technologies model WS-400A-6NPP) were 20s, 2000rpm.

Preparation of lignin film

A 1.0% lignin solution was prepared by dissolving MWL (Norway spruce) from Dr. Argyropoulos group with 1,4-dioxane. The solution was allowed to be dissolved for one day. A small part of high molecular weight particle was filtered by syringe filter (Millex®-FG, pore size 0.2μ). A few drops of the lignin solution were applied on the polystyrene coated QCM-D crystal and it was spin coated at 3000rpm for 20 seconds.

Results and Discussion

Morphology of the model surfaces

Figure 1 shows the AFM phase images of (a) polystyrene and (b) lignin deposited on polystyrene coated QCM-D Au crystal. Figure 1b shows the spincoated lignin surface. The RMS value of the lignin film is 2nm in 2 x 2 μm.

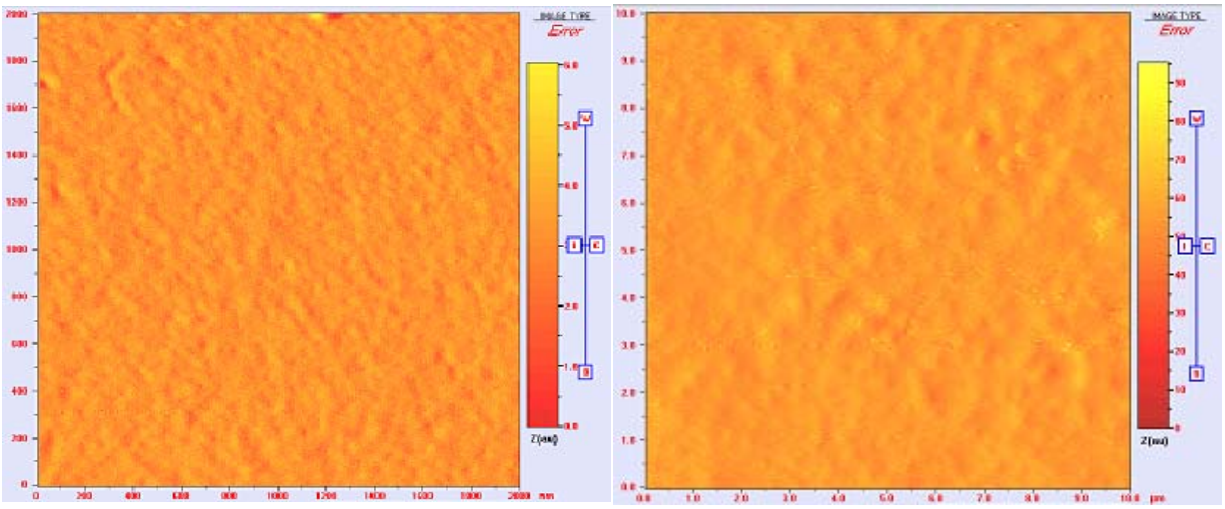

Fig 1. AFM phase images of (a) polystyrene (left) and (b) lignin on polystyrene surface (right).

QCM-D studies with the model surfaces

The frequency and dissipation changes upon laccase treatment are shown in Figure 2. First, a pH 4.5 buffer solution was injected into the QCM cell, where a lignin-covered QCM electrode was installed. At least 18 hours were allowed for the lignin to fully swell in the pH 4.5 buffer solution. After this stage, 0.5 ml of pH 10 buffer solution was introduced into the QCM cell with a syringe pump (Cole-Parmer 74900 series) at a flow rate of 0.2 ml/min.

When frequency curves were stabilized, 0.5ml of pH 4.5 buffer solution was injected at the same flow rate with the syringe pump. In a short time, the frequency curves reached a plateau and 0.5ml of the enzyme solution was injected with same method. Approximately, after 5 hours laccase treatment in situ, 0.5ml of pH 10 buffer solution was introduced by syringe pump at 0.2ml/hr flow rate. By comparing the two frequency changes before and after laccase treatment in a same condition (pH 10), it is possible to conclude that the laccase plays an important role to change the properties of lignin film. The significant change in frequency after the enzyme treatment can be caused by oxidation of lignin film with laccase. This mechanism is well documented in the literature [6].

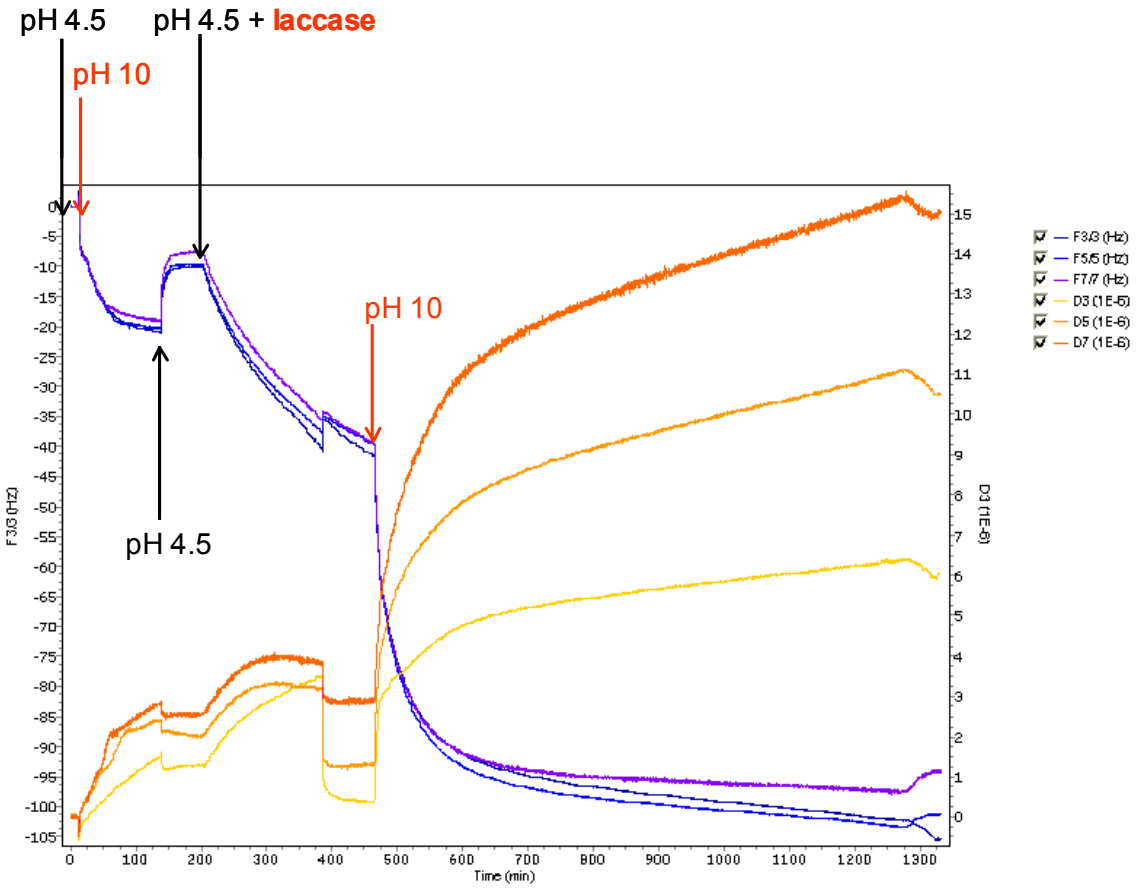

Figure 2. Change in frequency and dissipation by enzymatic treatment on lignin thin films in laccase solution (25°C, 25ppm enzyme concentration). The different lines represent the different overtones (harmonics): $f_3/3$ (navy blue line), $f_5/5$ (light blue), $f_7/7$ (purple), D_3 (yellow), D_5 (light orange) and D_7 (orange). The driving frequencies correspond to 15, 25 and 35 MHz for f_3, f_5 and f_7, respectively.

Contact Angle changes with model surface

A MWL lignin model surface was used to investigate contact angle changes as a function of the time of laccase treatment. Without laccase treatment, the angle on lignin surface was 85°. After 1 hour enzyme incubation, the contact angled changed significantly to 67°. The

contact angle was decreased to 55° in the enzyme treatment for 2 hours. It is clearly demonstrated that as the time of the laccase treatment increases, the lignin surface became more hydrophilic. However, the contact angle was insignificantly affected after 2 hours enzyme incubation. During overnight treatment, it was changed only to 48°.

Conclusions

A lignin (MWL) film was produced on a polystyrene coated QCM-D crystal. The enzymatic treatment caused significant swelling in alkaline condition. Such swelling effect was compared to the frequency and dissipation changes without laccase treatment and it was indicated that the hydrophobicity of lignin film was significantly decreased in the presence of laccase. The investigation on the contact angle changes with enzyme incubation supported the property changes of lignin model surface.

References

[1] S. Larsson, P. Cassland, L.J. Jonsson, "Development of a Saccharomyces cerevisiae strain with enhanced resistance to phenolic fermentation inhibitors in lignocellulose hydrolysates by heterologous expression of laccase," Applied and environmental Microbiology, vol. 67, pp. 1163-1170, 2001.

[2] M. Servili, G. Destefano, P. Piacquadio, V. Sciancalepore, "A novel method for removing phenols from grape must," American Journal of Enology and Viticulture, vol. 51, pp. 357-361, 2000.

[3] F. Carunchio, C. Crescenzi, A.M. Girelli, A. Messina, A.M. Tarola, "Oxidation of ferulic acid by laccase," Talanta, vol. 55, pp. 189-200, 2001.

[4] Y. Wong, J. Yu, "Laccase-catalyzed decolorization of synthetic dyes," Water research, vol. 33, pp. 3512-3520, 1999.

[5] P.M. Gelo, H.H. Kim, N.G. Butlin, G.T.R. Palmore, "Electrochemical studies of a truncated laccase produced in *Pichia pastoris*," Applied and environmental Microbiology, vol. 65, pp. 5515-5521, 1999.

[6] C. Crestini, L. Jurasek, and D. S. Argyropoulos, "On the Mechanism of the Laccase-Mediator System in the Oxidation of Lignin," Chemistry A European Journal, vol. 9, pp. 5371-5378, 2003.

[7] S. Kawai, M. Nakagawa, H. Ohashi, "Degradation mechanisms of a nonphenolic β-O-4 lignin model dimmer by *Trametes versicolor* laccase in the presence of 1-hydroxybenzortriazole," Enzyme and Microbial Technology, vol. 30, pp. 482-489, 2002.

[8] A. Castro, D. V. Evtuguin, A. Xavier, “Degradation of biphenyl lignin model compounds vy laccase of *Trametes versicolor* in the presence of 1-hydroxybenzotriazole and heterpolyanion,” Journal of Molecular Catalysis B: Enzymatic, vol. 22, pp. 13-20, 2003

Chapter 4.

Salt-induced depression of lower critical solution temperature in surface-grafted neutral thermoresponsive polymer

Introduction

Thermally responsive polymers exhibit measurable changes in their conformation as a function of temperature. The quintessence of this category of polymers is poly(N-isopropyl acrylamide) (PNIPAM), whose bulk phase transition temperature in aqueous solution, T_C, is ≈32 ^oC.[1] While below this temperature PNIPAM is soluble in water, upon raising temperature above 32 ^oC the polymer phase-separates from the solution. This temperature-dependent solubility change of PNIPAM has been cleverly used in a number of applications such as controlled drug delivery,[2,3,4] gene therapy,[5] and creation of reversible non-fouling surfaces[6,7,8] and artificial organs.[9] While the lower critical phase transition of free PNIPAM chains in aqueous solution has been extensively studied, the phase behavior of PNIPAM chains grafted to a solid substrate is relatively less explored. Surface plasmon resonance measurements by Lopez *et al.*[10] and neutron reflectively studies by Kent and coworkers[11,12,13] demonstrated that the phase transition of PNIPAM brush takes place over a broad range of temperature around 32 ^oC. Recent study by Zhang *et al.* utilizing quartz crystal microbalance with dissipation measurement (QCM-D) confirmed such broad transition of surface-grafted PNIPAM.[14,15] While temperature is certainly an important factor determining the response of a thermoresponsive polymer, the concentration of salt in the solution has also been found to affect the phase transition of free PNIPAM.[16]

Understanding the behavior of thermoresponsive polymer in solutions of varying salinity is crucial in order to utilize these polymers in biological applications.

In this communication, we employ QCM-D to probe the phase transition behavior of surface-grafted PNIPAM as a function of salt concentration in the solution. We demonstrate that the inverse relationship between the concentration of salt present in the aqueous solution and T_C observed for bulk PNIPAM also holds true for grafted polymers. However, this relationship is not linear as is observed for free PNIPAM in aqueous solutions. Specifically, at low salt concentrations T_C decreases more rapidly and tends to level off at elevated salinity of the solution.

Experimental Part

Attachment of PNIPAM to QCM resonator: Polished, AT-cut quartz crystals (1.4 cm in diameter), with a fundamental resonant frequency of 5 MHz were obtained from Q-Sense AB (Sweden). The active side of the crystal was coated with a thin layer (≈50 nm) of silicon oxide. PNIPAM chains were grafted from this layer of silicon oxide using atom transfer radical polymerization.[17] Thickness of PNIPAM on QCM crystal was estimated by growing PNIPAM brushes simultaneously on a reference silicon wafer and measuring the dry thickness of the polymer layer (≈15nm) by ellipsometry.

Data acquisition using QCM-D: The variations in frequency (Δf) and dissipation (ΔD) were monitored using a QCM-D apparatus (Q-Sense AB, Sweden) consisting of a pre-heating loop and a chamber connected to the electronic unit. (Δf) and (ΔD) were determined for bare crystals (*i.e.*, bare silica-coated resonators with no attached polymer) as well as for crystals coated with PNIPAM. The resonator was placed in the QCM chamber, with the

silica-coated side of the crystal facing the liquid and the other side exposed to air. In a typical experiment, the solution was conditioned in the heating loop before entering the chamber. The temperature of the liquid in the chamber was controlled within ±0.02 ^{o}C with a Peltier element. In order to understand the response of PNIPAM to external stimuli, solutions of different ionic strengths and different temperatures were circulated over the PNIPAM-coated surface of QCM crystals. Δf and ΔD were measured at a sampling rate of 1 Hz with a sensitivity of <0.5 Hz and $1x10^{-7}$ (au), respectively. While replacing the liquid present in the chamber, due care was taken to completely flush out the original liquid. For this purpose, a large volume of new solution was circulated through the chamber for 5 minutes, and then the outlet of the chamber was closed to fill it up with the solution of given salt concentration. For every new measurement, the PNIPAM-coated resonator was allowed to equilibrate for at least 45 minutes.

Results and Discussion

Investigating the response of grafted polymers to changes in environment has been historically challenging due to the lack of readily available, unambiguous surface characterization techniques. Although the thermoresponsive nature of free PNIPAM has been known since late 1960's,[18] systematic exploration of surface-grafted PNIPAM commenced only .[10,11,12,13] Consequently, there have been only a handful of studies that probed the responsive nature of PNIPAM brushes. Recently, quartz crystal microbalance with dissipation monitoring (QCM-D) has emerged as a sensitive probe to investigate phenomena taking place at or near surfaces.[14,15,19,20,21] Since the response of the quartz crystal is affected by variations in temperature, viscosity, and density of the (bulk) medium

above the sensor surface, the inherent crystal effects must be taken into consideration to obtain the true response of PNIPAM brushes. Consequently, we first measured Δf and ΔD for bare crystals at different temperatures and salt concentrations. These values were subtracted from the corresponding Δf and ΔD for PNIPAM-coated QCM crystals to obtain corrected Δf and ΔD for the grafted PNIPAM chains. In this communication, we report Δf and ΔD values with respect to those for DI water at 25 ˚C.

Figure 1 depicts Δf and ΔD for PNIPAM as a function of temperature when NaCl solutions with two different salt concentrations were circulated over the PNIPAM-coated resonator. Every data point in this graph was obtained after Δf and ΔD reached a steady value at a particular temperature.. Δf increases with increasing solution temperature, indicating a decrease in the effective mass of the adlayer attached to the resonator. Since the PNIPAM chains are chemically grafted to the crystal, the observed decrease in mass is explained by the loss of water molecules bound to PNIPAM chains. It has been previously shown that QCM is capable of sensing the mass associated with water molecules bound to the organic species *i.e.*, water of hydration. In fact, the ability of QCM to detect the degree of hydration of organic species results in a different mass sensed by this technique as compared to that sensed by other ones such as ellipsometry, surface plasmon resonance or optical waveguide light spectroscopy.[20,21] Consequently, we attribute the observed increase in Δf to the loss of water molecules bound directly to grafted PNIPAM chains.

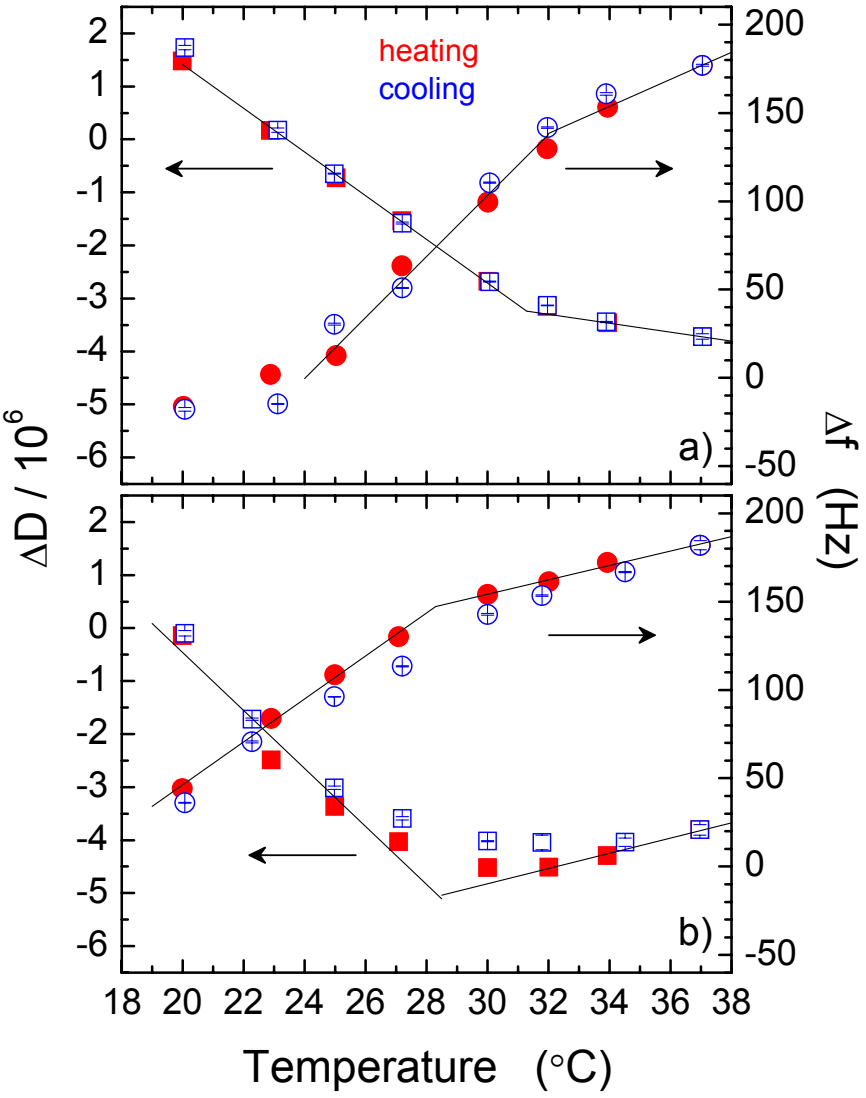

Figure 1 *ΔD* (squares, left ordinate) and *Δf* (circles, right ordinate) values measured on PNIPAAm brushes (dry thickness = 15 nm) in aqueous NaCl solutions having (a) 250 mM and (b) 1 M concentrations as a function of the solution temperature. Both the heating and the cooling cycles (red solid and blue open symbols, respectively) are shown. The standard deviation for each data point is represented as an error bar (in all cases smaller than the symbol's size)

Dehydration of PNIPAM results in gradual collapse of the grafted chains and a consequent decrease of the compatibility between PNIPAM and aqueous solution. This transition from fully solvated chains to a collapsed structure of PNIPAM brushes occurs over a wide range of temperature (from at least 20 to 37 ˚C). This is in contrast to the very sharp coil-to-globule transition, T_C, observed at 32 ˚C for free PNIPAM chains in solution. Thus, the confinement of thermally responsive chains to a surface seems to affect its thermal transition behavior. Our results agree very well with those obtained by Lopez *et al.* using surface plasmon resonance, by Kent *et al.* using neutron reflectivity, [10, 11,12,13] and by Zhang *et al.* using QCM-D.[14,15] These investigations also pointed at a gradual transition of surface-grafted PNIPAM over a wide range of temperature..

It is expected that the viscoelastic properties of grafted PNIPAM will change upon dehydration and shrinking of these surface-anchored brushes. Specifically, a decrease in the values of ΔD reflects the gradual variation in energy dissipation (viscoelasticity) of the PNIPAM layer as temperature is increased (*cf.* Figure 1). A dense and compact layer is known to result in less energy dissipation (ΔD) relative to an extended and flexible one.[20,21] By combining Δf and ΔD measurements, the following picture of PNIPAM phase transition emerges. Upon increasing temperature PNIPAM chains begin to lose water of hydration and the incompatibility between chains and aqueous solution increases. This incompatibility causes the chains to collapse, which in turn, makes the layer compact, resulting in a decrease in dissipation.

We repeated the above experiments at different salt concentrations by flowing different salt solutions over PNIPAM-coated crystals. In all the experiments, we detected variations in Δf and ΔD similar to those observed in Figure 1. However, at a given temperature, Δf increased

and ΔD decreased as salt concentration was increased. As Δf is correlated with loss of water of hydration, we postulate that at 25 ^{o}C grafted PNIPAM chains lose more water of hydration than the ones in contact with solutions of lower salt concentration. Similar results were obtained upon measuring the deviation of D as a function of salt concentration (*cf.* Figure 2). At a given temperature, ΔD decreases as the ionic strength of the solution is raised. As dense and compact layers exhibit lower D than flexible layers, we hypothesize that at 25 °C PNIPAM brushes are more collapsed in solutions having higher concentrations of salt. We can use the experimentally measured Δf and ΔD to estimate the changes in T_C as a function of the salt concentration.

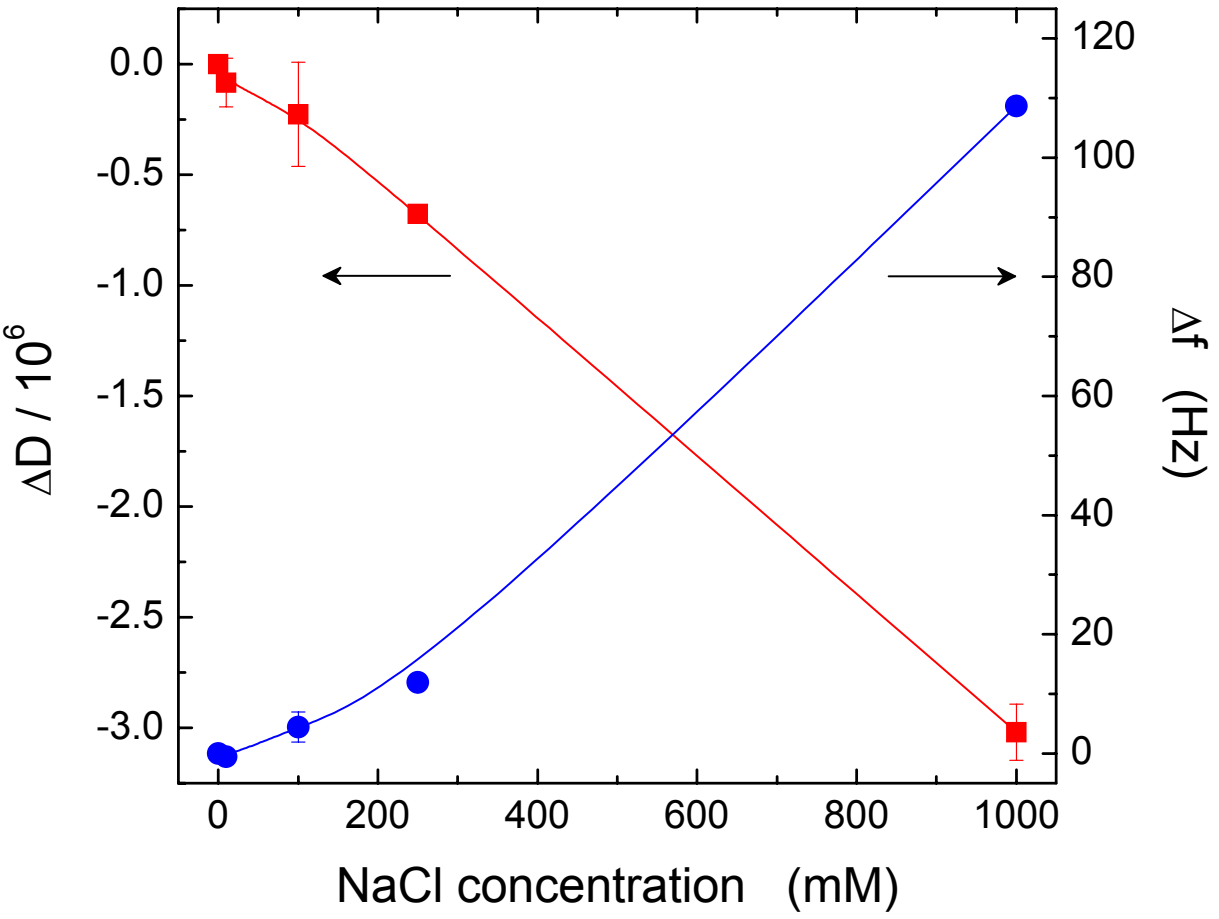

Figure 2 *ΔD* (squares, left ordinate) and *Δ*f (circles, right ordinate) values measured on PNIPAAm brushes (dry thickness = 15 nm) at 25.00±0.02°C as a function of the concentration of NaCl in solution. The reference data point is deionized water, pH=5.5 at 25 °C. The lines are meant to guide the eye

Since the phase transition of grafted PNIPAM is not as sharp as that for free polymers, we determined the extent of phase transition of surface-anchored PNIPAM by following Δf (or ΔD) as a function of temperature. We define T_C of grafted PNIPAM, $T_{C,graft}$, to be the

temperature at which the slope of Δf (or ΔD) changes in plots similar to those shown in Figure 1. While the value of $T_{C,graft}$ determined using this approach is physically not as definitive as T_C for free PNIPAM, it provides a quantitative estimate to compare phase transition behaviors of grafted polymers under various solution conditions. Our results (*cf.* Figure 3) reveal that $T_{C,graft}$ decreases with increasing salt concentration.

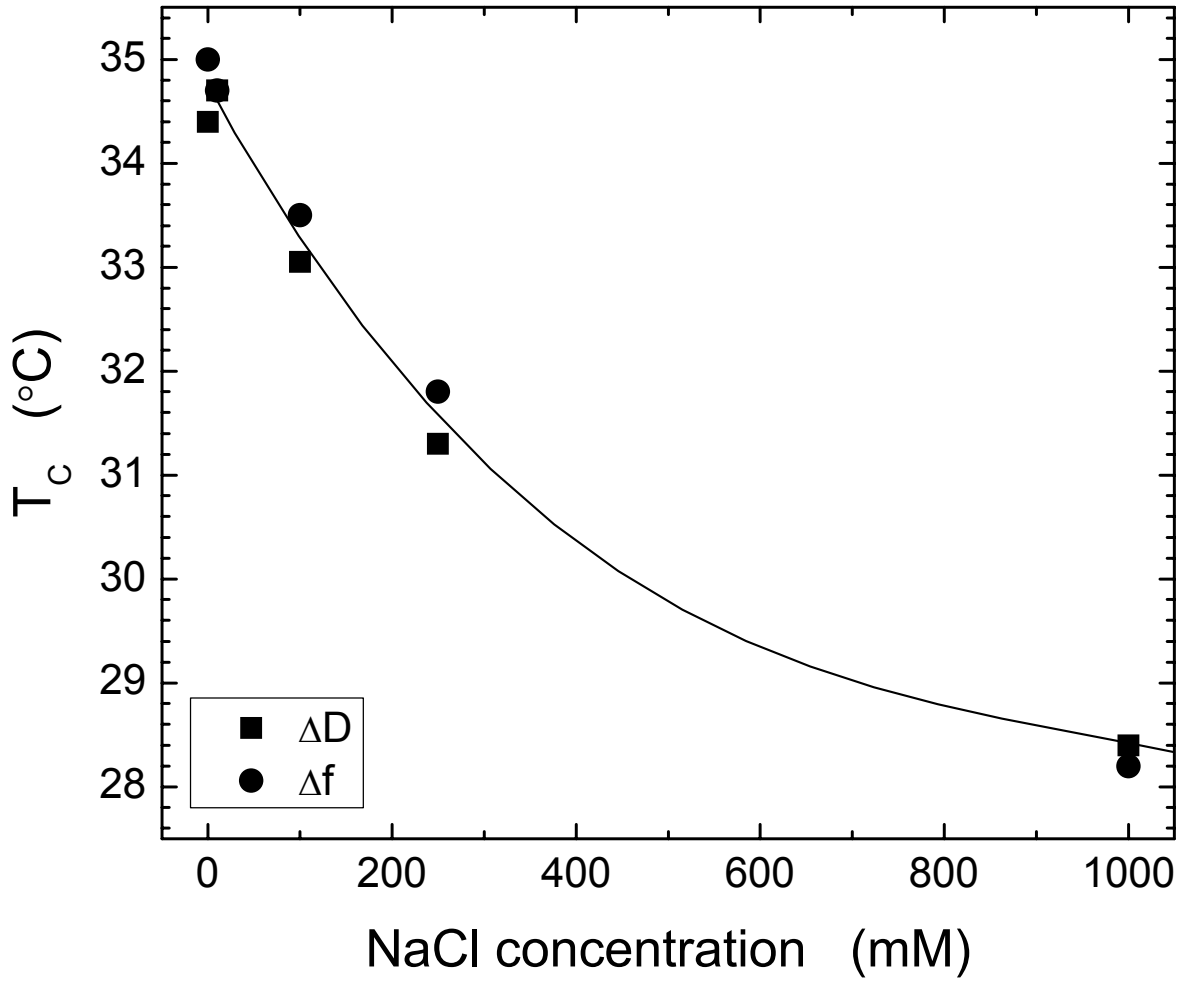

Figure 3 The coil-to-globule transition temperature in PNIPAAm brushes ($T_{C,graft}$) as determined from the temperature dependent dissipation (squares) and frequency (circles) data as a function of the concentration of NaCl in solution. The line is meant to guide the eye.

These observations are in line with the earlier experiments that described depression of T_C of bulk, free PNIPAM upon increasing salt concentration.[16] This effect of salt was attributed to

the ability of inorganic ions to either make or break the structure of water molecules in the solution (Hofmeister effect).[16,22] One of the reasons proposed to explain phase transition of PNIPAM is the minimization of structural deformation of water molecules around hydrophobic isopropyl groups in PNIPAM. Addition of salt can change the structure of water in their vicinity and consequently influence the hydration of the hydrophobic groups. Structure makers such as NaCl cause water molecules to form a "rigid" structure around the ions. This reduces the hydration of the hydrophobic groups along PNIPAM chain and results in the lowering of T_C.[16]

While there can be other plausible reasons explaining the effect of salt on PNIPAM such as direct interaction of ions with amide groups in the polymer,[16c] our observation that addition of salt affects phase transition of thermoresponsive polymer brushes still remains valid. It is worth noting that although the surface-grafted PNIPAM shows similar trends in T_C depression as free PNIPAM, the trend is distinctively not linear for grafted PNIPAM. A relatively rapid decline in $T_{C,graft}$ is seen upon increasing the salt concentration up to 250 mM; further increase in NaCl concentration does not produce decline in $T_{C,graft}$ at such a rate. This effect may be associated with the loss of translational entropy of the grafted chains relative to the free macromolecules. Tests to prove this hypothesis are underway using PNIPAM brushes with different grafting densities on the substrate.

Conclusions

By using quartz crystal microbalance with dissipation monitoring, we probed the phase transition behavior of thermoresponsive polymer brushes (PNIPAM) immersed in aqueous

solutions at various salt concentrations. The phase transition temperature of grafted polymer, $T_{C,graft}$ as defined in the text, was found to decrease as the concentration of salt is increased. This depression in phase transition temperature is similar to that observed for free PNIPAM and is attributed to the effect of salt ions on water molecules around polymer chains (Hofmeister effect). However, unlike free PNIPAM, the depression of Tc for PNIPAM brushes is not linear as a function of salt concentration.

References

[1] H. G. Schild, *Prog. Polym. Sci.*, **1992**, 17, 163.

[2] J. Kost and R. Langer, *Adv. Drug Deliv. Rev.*, **2001**, 46, 125.

[3] D. Neradovic, W. L. J. Hinrichs, J. J. Kettenes-Van Den Bosch, C. F. Van Nostrum and W. E. Hennink, *J. Contr. Rel.*, **2001**, 72, 252.

[4] T. Inoue, G. H. Chen, A. S. Hoffman and K. Nakamae, *J. Bioact. Compat. Polym.*, **1998**, 13, 50.

[5] M. Kurisawa, M. Yokoyama and T. Okano, *J. Contr. Rel.*, **2000**, 69, 127.

[6] N. Yamada, T. Okano, H. Sakai, F. Karikusa, Y. Sawasaki and Y. Sakurai, *Makromol. Chem. Rapid Commun.*, **1990**, 11, 571.

[7] L. K. Ista and G. P. Lopez, *J. Ind. Microbiol. Biotechnol.*, **1998**, 20, 121.

[8] D. Cunliffe, C. D. Alarcon, V. Peters, J. R. Smith and C. Alexander, *Langmuir*, **2003**, 19, 2888.

[9] N. Angelova and D. Hunkeler, *Trends Biotechnol.*, **1999**, 17, 409.

[10] S. Balamurugan, S. Mendez, S. S. Balamurugan, M. J. O'Brien, G. P. Lopez, *Langmuir*, **2003**, 19, 2545.

[11] H. Yim, M. S. Kent, S. Satija, S. Mendez, S. S. Balamurugan, S. Balamurugan, G. P. Lopez, *Phys. Rev. E*, **2005**, 72, Art. No. 051801.

[12] H. Yim, M. S. Kent, S. Mendez, S. S. Balamurugan, S. Balamurugan, G. P. Lopez, S. Satija, *Macromolecules*,**2004**, 37, 1994.

[13] H. Yim, M. S. Kent, D. L. Huber, S. Satija, J. Majeswski, G. S. Smith, *Macromolecules*, **2003**, *36*, 5244.

[14] G. Zhang, *Macromolecules*, **2004**, 37, 6553.

[15] G. Lui and G. Zhang, *J. Phys. Chem. B*, **2005**, 109, 743.

[16] [16a] H. G. Schild and D. A. Tirrell, *J. Phys. Chem.*, **1990**, 94, 4352; [16b] H. Inomata, S. Goto, K. Otake and S. Saito, *Langmuir*, **1992**, 8, 687; [16c] T. G. Park and A. S. Hoffman, *Macromolecules*, **1993**, 26, 5045; [16d] R. Freitag and F. Garret-Flaudy, *Langmuir*, **2002**, 18, 3434; [16e] Y. Zhang, S. Furyk, D. E. Bergbreiter and P. S. Cremer, *J. Am. Chem. Soc.*, **2005**, 127, 14505.

[17] K. A. Davis, K. Matyjaszewski, *Adv. Pol. Sci.* **2002**, *159*, 1

[18] M. Heskins, J. E. Guillet, *J. Macromol. Sci.*, **1968**, 2, 1441.

[19] S. E. Moya, A. A. Brown, O. Azzaroni, W. T. S. Huck, *Macromol. Rapid Commun.*, **2005**, 26, 1117.

[20] F. Hook, M. Rodahl, P. Brzezinski and B. Kasemo, *Langmuir*, **1998**, 14, 729.

[21] F. Hook, B. Kasemo, T. Nylander, C. Fant, K. Sott and H. Elwing, *Anal. Chem.*, **2001**, 73, 5796.

[22] [22a] P. H. von Hippel and T. Schleich, *Acc. Chem. Res.*, **1969**, 2, 257; [22b] H. S. Frank and W. Y. Wen, *Discuss. Faraday Soc.*, **1957**, *24*, 133.

Chapter 5. OVERALL CONCULSIONS

(1) A QCM technique was used to assay the activity of cellulose, probe the phase transition behavior of polymer brushs (PNIPAM) and investigate the hydrophilicity of milled wood lignin was performed with model polymeric thin films. The initial slope in frequency vs time curves was related to the initial reaction rates and it was effective to estimate enzyme performance under different conditions temperature, pH, and concentration.

(2) The phase transition temperature of grafted polymer (PNIPAM) was found to decrease as the concentration of salt is increased. This depression in phase transition temperature is attributed to the effect of salt ions on water molecules around polymer chains (Hofmeister effect).

(3) The laccase incubation caused significant swelling of lignin film in alkaline condition. It was demonstrated that the hydrophilicity of lignin surface was significantly ameliorated in the presence of laccase.

Chapter 6. SUGGESTED FUTURE WORK

(1) Pure cellulase system can be recommended to estimate clear enzyme adsorption kinetics.

(2) Surface Plasmon Resonance technique can be used to investigate lignin degradation with laccase-mediator system